REDUCING URBAN HEAT ISLANDS AND IMPROVING THE THERMAL COMFORT OF RESIDENTS – A NATURE-BASED SOLUTION

UDK: 711.4(536.21)
502.131.1
DOI: 10.5937/a-u0-27685
COBISS.SR-ID: 41438729

РЕДУКЦИЈА УРБАНИХ ТОПЛОТНИХ ОСТРВА И ПОБОЉШАЊЕ ТОПЛОТНОГ КОМФОРА СТАНОВНИКА - РЕШЕЊЕ ЗАСНОВАНО НА ПРИРОДИ

Оригиналан научни рад, рад примљен: јул 2020., рад прихваћен: фебруар 2021.

Томислав Ђорђевић*

ABSTRACT

The benefits of urban blue-green infrastructures are well known: they intercept airborne three-atom particles, thus reducing pollution levels; and they provide shade and cooling by means of evapotranspiration. The focus of this paper is to demonstrate methods such as remote sensing and multi-spectral analysis, which can be a very useful addition to the quantification of blue-green infrastructures for cooling and shading, especially in the highly complex geometry of city blocks. The basic aim of this research is to attempt to reduce urban heat islands and in this way to indirectly increase the comfort of living. A cause/effect relationship between the envelope of built up structures and the solar radiation distribution on the environment was established by means of mulit-spectral analysis, and an estimation was made concerning the lack of vegetation on a specific parcel/block (an important tool for urban planners).

This state-of-the-art methodology was applied to the optimized prediction concept of vegetation resources. Now it is possible to create a model that will incorporate this newly-added urban vegetation into urban plans, depending on the evaporation potential that will affect the microclimate of the urban area. Such natural cooling can be measured and adapted and hence aimed at a potential decrease in temperature in areas with UHI emissions.

As a case study, part of a seacoast urban block (Abu Dhabi UE,) was analysed with and without a street treeline and green façades and roofs. It was concluded that green infrastructure reduced the land surface temperature by up to 4.5˚C.

Key words: urban heat islands (UHI), land surface temperature (LST), land use and land cover (LULC), normalized difference vegetation index (NDVI)

АПСТРАКТ

Предности урбане плаво-зелене инфраструктуре добро су познате: елиминишу троатомске честице у ваздуху – смањују ниво загађења, омогућавају засенчење и природно хлађење евапотранспирацијом. Фокус овог рада је примена релативно нових метода даљинске детекције и технике мулти-спектралне анализе, које су врло користан додатак квантификацији плаво-зелене инфраструктуре, ради природног хлађења и засенчења, посебно у изузетно сложеној геометрији градских блокова. Основни циљ овог истраживања је покушај да се смање ефекти урбаних топлотних острва и да се на тај начин индиректно утиче на побољшање животног комфора. Мулти-спектралном анализом утврђени су узрочно-последични односи изграђене физичке структуре (зграде и инфраструктура) и расподеле сунчевог зрачења на непосредну животну околину, као и процена недостатка вегетације на нивоу парцеле/блока (важан урбанистички алат).

Иновативна метода оптимизације вегетативних ресурса примењена је на предикционом концепту урбаног модела. Сада је могуће креирати модел који ће квантификовати евапоративни потецијал новопланиране вегетације у зависности од енергије испаравања лишћа, што ће имати утицаја на микроклиму градског подручја. Такво природно хлађење може се мерити и прилагодити, а тиме и усмерити ка потенцијалном смањењу топлотне емисије делова подручја са урбаним топлотним острвима (UHI).

Ова студија случаја односи се на урбани блок непосредно уз обалу мора (Абу Даби, УЕ,) који је анализиран у опцији са и без уличних дрвореда, односно зелених фасада и кровова. Закључено је да урбано зеленило редукује температуру површине тла (LST) до 4,5 оС.

Кључне речи: урбана топлотна острва (UHI), температура површине земљишта (LST), намена земљишта (LULC), оптимални количник вегетативног индекса (NDVI).

* Др Томислав Ђорђевић дип.инж.арх, Научни сарадник у European Center for Peace and Development (ECPD), established by the United Nations University for Peace, Теразије 41, Београд, стално запослен у EXPO AG Biro doo, Лазаревачка 2а, Београд у својству пројектанта, tdjordjevic99@gmail.com

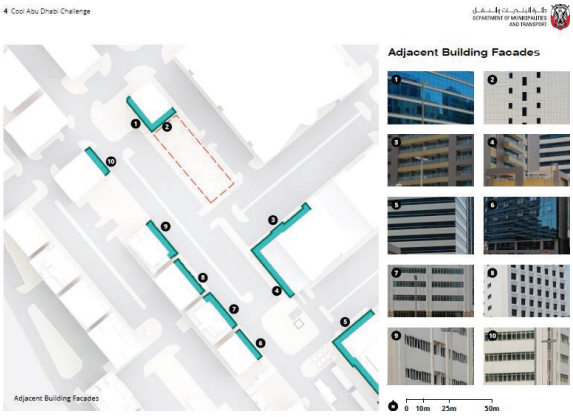

Fig. 1. City site, with existing building façade / Сл.1. Градска локација са постојећим изгледима зграда

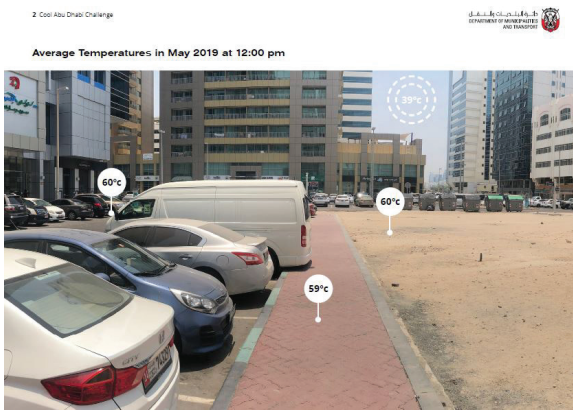

Fig. 2. Average temperature in May 2019, 12:00 pm / Сл.2. Просечна температура мерена у подне за мај 2019 године

INTRODUCTION

For the purposes of this study, innovative, state-of-the-art technology was implemented. There have been a number of theoretical and experimental studies (regarding spectral wavelengths) that aim to quantify land surface temperature (LST) and land use and land cover (LULC) (e.g., Alshaikh, 2015; Kalma et al., 2008; Milanović and Filipović, 2017). However, the novelty of this study lies in remodeling urban areas with higher LST, which was then implemented on the project model with lower LST vegetation patches. These classifications were synthetised through repeated multispectral analysis, which resulted in a temperature change and a reduction in urban heat islands. Such cooling effectiveness can be measured and adapted, and hence facilitate green infrastructure corridors aimed at a potential decrease in urban heat island (UHI) emissions. Using remote sensing, it is now possible to create a prediction model that will incorporate urban vegetation into space depending on the evaporation potential of the leaves, which takes into account the canopy, wind direction, humidity, irrigation of plants, and the physical urban shape (buildings and infrastructures) that will affect the microclimate of the urban area. By implementing the geospatial method of remote sensing, it is possible to analyse and quantify the impact of over-building on the rise temperatures in urban areas, as well as the disturbance of the heating comfort and the increasing demands for additional cooling. By implementing the method of multispectral analysis of satellite images on the city's urban block and its contact with the bordering areas, a possible development with regard to UHI will be shown (Noyingbeni et al., 2016).

By analysing the cause/effect relationship between building envelopes (high-rise) and the distribution of solar radiation on the environment, we estimated that the amount of green vegetation is a regulating factor in the micro-climate of inner city areas. Appropriate greenery in the summer season can be an effective enhancement, which at the same time enables and supplements several cooling mechanisms, namely, evaporative cooling and evapotranspiration, i.e. natural cooling systems. The remote sensing and method of calculating the Normalised Difference Vegetation Index (NDVI) (Bannari, et al., 1995; Garbulsky, et al., 2011) was used to establish and classify a map of the healthy and unhealthy greenery zones, that is the vegetation zones with the highest evaporative potential, which can be incorporated in the urban prediction model.

The reclassification method was used in the following way: a certain spectral wavelength (reflected in the near_ infra_ red (NIR) range of the classification for healthy greenery) was implemented on the prediction model, as was the lowest temperature range of that zone. The synthesis method was applied on the LULC to determine the new reduced temperature range (LST), which modified the model.

The energy model applied in the research served to confirm the remote sensing results, as summer solar exposure in the urban area strongly increases energy consumption, especially for high building densities. This study analysed how the energy consumption and morphology of buildings are in relation to the surrounding environment (like humidity, airspeed, the shape of buildings), and how they cause local variations of microclimate (Milanović and Filipović, 2017).

CASE STUDY

This article is a digest of a paper titled A Nature-based Solution, which was an entry (by the author of this article and his team) to an international contest announced by the City of Abu Dhabi[1] in early 2020 (Cool Abu Dhabi Challenge)[2]. The subject of the contest was to propose a solution for the heat problems relating to a site – a typical Abu Dhabi downtown block – which contains a small open plaza surrounded by a surface parking lot that is abutted by 15-story buildings on all sides (Fig. 1 and Fig. 2). The ground cover is dominated by asphalted streets with precast curbs and cast pavers. Very little vegetation exists directly on the site. The temperature on the site was shown on an exact date – May 16, 2019 at 12:00 pm.

1 The Winning Entries and Honorable Mentions can be viewed on the official website here: https://www.coolabudhabi.com/#winning-entries and on social media here: https://twitter.com/admediaoffice/status/1313449546148610050

2 The Department of Municipalities and Transport of Abu Dhabi invited architects and engineers to participate in global creative ideas competition to improve outdoor thermal comfort in the public space by mitigating the impact of the Urban Heat Island Effect in the city. The deadline was May 12, 2020. More than 1000 teams from 67 countries took part in the competition.

Fig. 3a (above) Landsat 8 scene coverage; Fig. 3b (middle) broader city zone; Fig. 3c (below) location of the hypothetical model / Сл. 3а (горе) сателитски снимак са Ландсат-а 8; Сл. 3б (средина) шира градска зона; Сл. 3в (доле) локација задатог хипотетичког модела

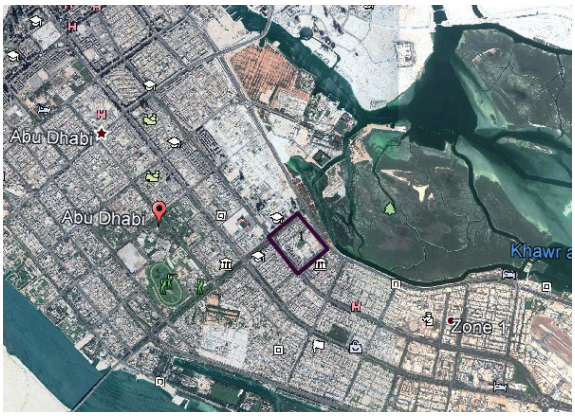

The focus of the research and the nature-based design solutions were to answer two basic questions:

- What is the relationship between urban blue-green infrastructure and urban thermal comfort?
- How does this concept reduce urban heat islands and improve the thermal comfort of the residents?

Study area

The broader area of interest is the central part of the city of Abu Dhabi. The area extends between the following geographic coordinates (EPSG: 4326): 54.3025181920000009E 24.3943239429999998N and 54.4511079589999980E 24.4965771175487355N (Figure 3).

Geospatial methods and analysis

With regard to the timeframe of the study, the data from satellite Landsat 8 (Fig. 3 a,b,c), bands: RGB+NIR (B2,B3,B4,B5) and TIRS: (TR 10+TR 11), which allow acquisition in the visible spectrum, were used, near infrared and thermal range. The address of the digital image according to the official information for Landsat 8 mission[3] is: C08_L1TP_160043_20190516_20190521_01_T1.

The basic specifications for the Landsat 8 data were GeoTIFF as the output format, and they were resampled using the Cubic Convolution method in a pixel size of 30 or 60 m, while the Universal Transverse Mercator (UTM) was used for the map projection and the World Geodetic System (WGS) 84 as the datum[4].

The multispectral bands applied were initially processed as Level 1 data and delivered in a 16-bit unsigned integer format. The data were rescaled at the top of the atmosphere (TOA) reflectance and TOA brightness temperature, with a 30 m spatial resolution as set in the research. Yuan and Bauer (2007) proposed a method for deriving the surface temperature (LST) in two steps: First, digital numbers (DNs) are converted to brightness. Second, radiation is converted to surface temperature using Landsat's specific estimate of Planck's Inverse law.

The TOA brightness temperature and Land Surface Temperature (LST) were calculated by applying the inverse of the Planck function3 and the arithmetic mean of the LST from TIR bands (10 and 11).

Satellite data processing

The first step in the processing of thermal satellite images was the conversion of DN pixel values into at-sensor spectral radiance. The conversion was done using the following formula:

1) $L\lambda = ML*DN+AL$,

where: L_λ is the spectral emission registered at sensor (Watts/(m2 *srad * μm); M_L is a multiplicative scale factor from the metadata (REFLECTANCE_MULT_BAND_x, where x is the band number); A_L is an additive scale factor from the meta data (REFLECTANCE_ADD_BAND_x, where x is a band number).[5]

The second step was to convert the reflectance to the atmospheric temperature over the land surface, according to the USGB hand book:

2) $T = K2/ln(K1L\lambda+1)-273.15$ (*Planck's inverse equation*)

where: K1 and K2 are radiation constants from the metadata, and is the effective wavelength.

3 (URL: https://www.usgs.gov/land-resources/nli/landsat)

4 (URL: https://www.usgs.gov/land-resources/nli/landsat/landsat-level-1-processing-details)

5 Based on Planck's law. https://www.usgs.gov/media/files/landsat-8-data-users-handbook

Metada data from Landsat images: K1 and K2 values for Landsat 8 thermal bands:

K1_CONSTANT_BAND_10 = 774.8853

K2_CONSTANT_BAND_10 = 1321.0789

K1_CONSTANT_BAND_11 = 480.8883

K2_CONSTANT_BAND_11 = 1201.1442

The following calculation was used: arithmetic mean for LST (the average of a set of numerical values for LST band 10 and LST band 11). This calculation based on the arithmetic mean gives better precision as compared to single-band values. As a side note, there are two methods for calculating the emissivity of each pixel of the NDVI classification. One is "split windows" and the other is "single windows".

3) The "single window" model was used:

Land surface temperature= BT/1+w*(BT/p)*ln(e))

Where:

- BT=At satellite temperature
- W=wavelength of emitted radiance (11μm)
- q=h*c/s(1.438-10^-2mK)
- h=Planck's constant (6.626*10^-34J/K)
- s=Boltzmann constant (1.38*10^23J/K)
- c=velocity of light (2.998*10^8m/s)

For Landsat 8, w=10.8, and equation p=h*s*c=14380, BT is T from step 2), actually the atmospheric temperature. The emissivity was calculated as shown in the description.

It is clear that each type of earth land cover has a different emissivity that is influenced by the instant physical state of the object. Therefore, it is important that the value of ε is measured at the time of the passage of the satellite platform for each individual image. Since we not have such field measurements, we needed to use one of the methods already described to calculate this parameter. An average value (based on the published measurements of spectral libraries) for each type of land surface was assigned to the classification method. Therefore, the method of calculating NDVI (Normalised Difference Vegetation Index) was used. For the Landsat images, we used threshold values for NDVI as follows:

If NDVI <0.2 type of land cover is considered soil, and ε = 0.97;

If NDVI> 0.5 type of land cover is considered vegetation, and ε = 0.99;

If 0.2 ≤ NDVI ≥ 0.5 type of land cover is considered mixed,

The equation for calculating NDVI (vegetation index) was:

$$\mathrm{NDVI} = \frac{NIR - RED}{NIR + RED}$$

The range lies between -1 and 1 so that the values from -1 to 0 relate to the urban area and from 0 to 1 – to natural vegetation.

3.1) $\varepsilon = mPv + n$,

where:

P is the proportion of vegetation and is emissiveness

3.2) $P = (NDVI + NDVImin/NDVImax - NDVImin)^2$

3.3) $\varepsilon = 0.004Pv + 0.986$

RESULTS AND DISCUSSION

Due to the pixel sizes of the bands (30m) and for this conceptual level, the existing data were not sufficient to draw adequate conclusions, and therefore the hypothetical model was rescaled (x 4.2) and resampled in the GIS analysis as reflection and brightness data recorded by the sensor (mostly Brightness Temperature, Surface Reflectance and related indexes), and also by calculating the Normalized Difference Vegetation Index (NDVI). The hypothetical model was analysed with regard to Abu Dhabi's hydro-meteorological features (temperature, atmospheric pressure, humidity and wind direction and velocity), the thermal characteristics of the buildings, and partly to the fluid dynamic (street canyon method) conditions and major vegetative evaporative potential, in order to evaluate the accuracy of the derived temperature values, which are relevant for the validation of the LST extraction. All errors that occured in this project are scale errors (with respect to pixel size 30/30m).

The Solution

Figures 4–6 are a detailed presentation of the influence of the land cover type and the changes in LULC. High absorption of wavelengths of visible red and strong reflection in the near infrared (NIR) region are due to chlorophyll found in vegetation, which mostly absorbs red light and reflects green (hence the green colour) (Kojović, 2013). Figure 4 presents the changes and the dynamics of the surface temperature, and an NDVI range of 0.6-0.8 indicates the presence of trees, while the isotherm indicates a lower temperature of 30–32˚C. LULC is presented using several classes (range: -1 to 0, artificial features and water bodies; 0.2 to 0.4, bare soil and grass; 0.6 to 0.8, variety of forest):

The NDVI images are a processed index of vegetation ranging from 0 to 1. The forest, with good evaporation, is marked as dark green (ranging from 0.6 to 0.8) and it generates temperatures in the range of 30-32˚C. The difference between the temperature of the buildings and the dark green vegetation is about 10˚C. The average temperatures by NDVI indicate that water bodies and forest plants operate as corrective factors for mitigating pollution at extreme temperatures created in urban space. An indicative limit for mitigating the urban climate is the urban forest temperature of 30-32˚C. If we manage to insert all the vegetation ranging from 0.6 to 0.8 and simulate approximately the same environment in our hypothetical model, we will be able to reach the above-mentioned maximum goal.

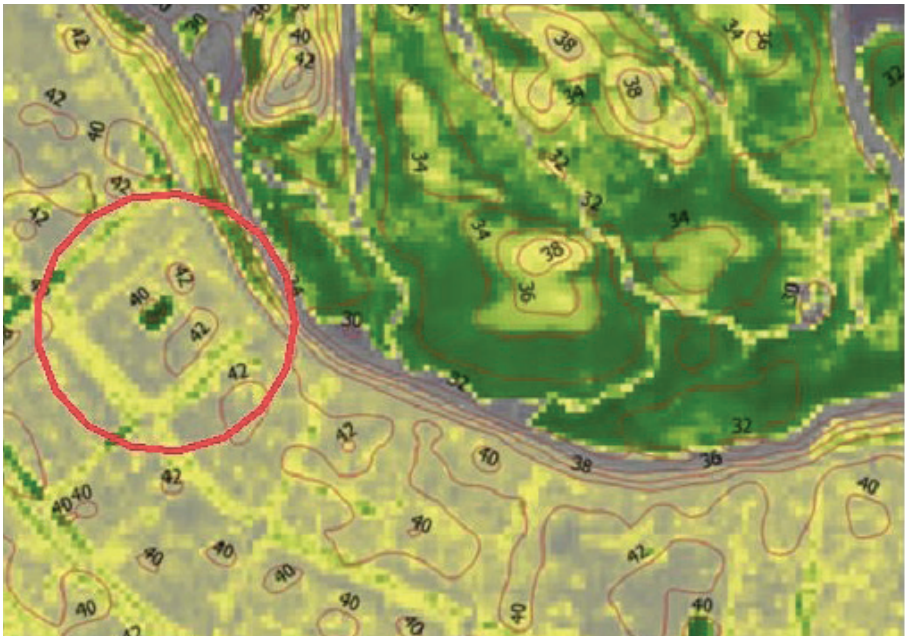

Fig. 4. NDVI range from -1 to 1. The red circle indicates the wider location of the block.
Сл. 4. NDVI ненадгледана класификација опсег од -1 до 1. Црвени круг означава ширу локацију блока

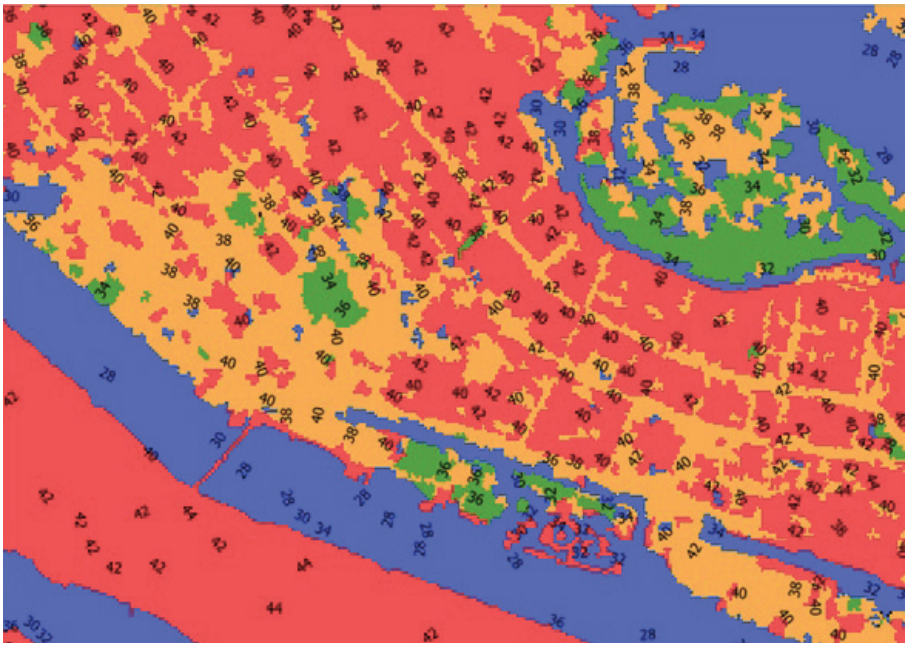

Fig. 5. LULC monitored classification
Сл. 5. LULC надгледана класификација

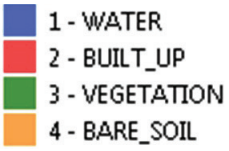

Fig. 6. LST with isotherms
Сл. 6. LST са изотермама

The results of this process, showing the average temperatures by classes, are given in Table 1. It is now possible to detect the UHI and determine the type of land use which causes this temperature effect:

Forest plants are an important source of adiabatic cooling and, if appropriately integrated into an urban space, represent a corrective factor for thermal accumulation and the emissions of the built physical structures. Evapotranspiration is the physical evaporation that accompanies photosynthesis. Not all tree species have the same effect of adiabatic cooling: The lower the temperature of the leaves, the higher the cooling (Alshaikh, 2015). All types of vegetative evaporative potential (deciduous trees) and environmental conditions on the site indicated within a range of 0.6-0.8 NDVI ought to be researched before being implemented into real situation. The results from May 16, 2019, for the broader city area of Abu Dhabi, show that the LST responds to the evapotranspiration of vegetation through internal and external thermodynamic energy conduction processes. The soil surface (covered by vegetation, mostly forest) has high evapotranspiration potential, and releases the energy absorbed as latent heat, resulting in low LST levels. Thus, the LST level is strongly determined by the vegetation cover, as well as by the soil moisture.

Urban transformation of the study area

The prediction for the future is modelled in this study, as an example of good practice. An urban reconstruction model could be designed to be compatible with the detailed urban plan (Đorđević et al., 2019). The hypothetical[6] plan was used as the base layer for the prediction model in a real situation for the new space modelling.

The coordinate reference system used for the analysis is: UTM 40N zone with WGS 84 datum (EPSG: 32640). The hypothetical block given (Fig. 7a) was shown within the real area (Fig. 7b).

The available official information on land use mapping and LST (Fig. 8 and Tab. 2) is more effective with the application of GIS modelling. The existing state of LULC is determined as a new layer for the prediction analysis.

This basis was used for the comparison and interpolation of the new building envelopes, a new garage, plenty of greenery, etc. In the prediction model, reclassification was carried out by replacing bare land and building façades with quality forest greenery in the parcels around the buildings and along the thoroughfares (Fig. 9a). A classification model was made using the new spatial data (Fig. 9b).

6 The hypothetical block was set by the Abu Dhai commission with alterations in the structure of objects, and does not fully correspond to the existing urban block.

Tab. 1 LST and LULC analysis / Таб. 1 *LST и LULC анализа*

Temp	Not categorized	Water m²	Built-up m²	Vegetation m²	Bare soil & built-up m²
26	0	95,651	0	0	0
27	1,993	20,716,417	0	0	0
28	0	19,451,034	19,927	0	0
29	0	5,123,308	11,956	0	33,876
30	0	3,614,811	67,753	111,593	426,444
31	0	3,140,542	249,091	765,208	729,339
32	0	2,656,309	360,684	1,269,369	876,801
33	3,985	1,934,940	727,346	709,412	765,208
34	1,993	1,169,732	1,068,103	557,964	729,339
35	21,920	625,717	1,402,882	623,724	1,020,278
36	13,949	322,822	1,861,209	514,124	1,365,020
37	1,993	227,171	2,166,097	322,822	1,809,398
38	5,978	191,302	3,015,000	276,989	2,496,890
39	1,993	203,258	6,386,698	181,338	4,714,798
40	0	169,382	14,395,479	45,833	6,406,626
41	1,993	103,622	16,440,019	13,949	3,826,041
42	3,985	61,775	12,038,080	0	1,337,122
43	5,978	121,557	7,365,129	0	559,957
44	3,985	21,920	1,402,882	0	304,888
45	0	0	292,931	0	400,539
46	0	0	87,680	0	37,862
47	0	0	7,971	0	0
Σm²	**69,745.5**	**59,951,270.0**	**69,366,917.4**	**5,392,326.3**	**27,840,425.2**
	Total m²				**162,620,684.5**
		Average temperature per class (°C)			
		30.4	**40.4**	**38.2**	**39.3**

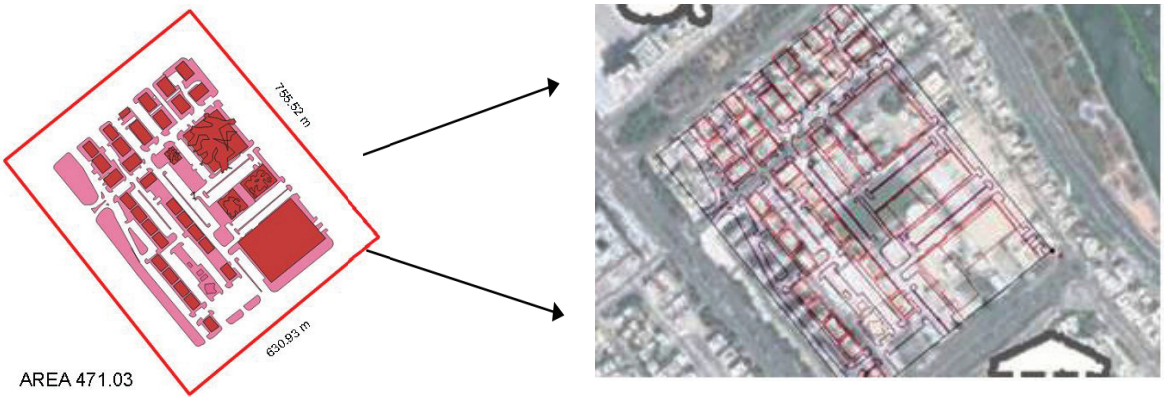

Fig. 7a (left) base layer (scaled x4.2 and rectified); Fig. 7b (right) base layer overlay with Google Earth image / Сл. 7а (лево) ситуација (увећана x4,2 и ректификована); Сл. 7б (десно) геопозиционирана ситуација прекопљена са Гугл мапом

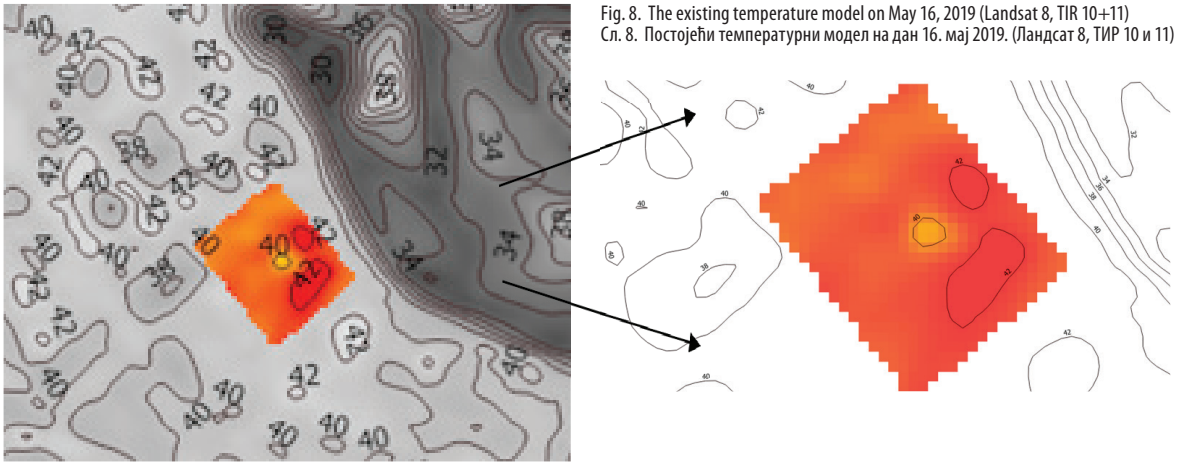

Fig. 8. The existing temperature model on May 16, 2019 (Landsat 8, TIR 10+11)
Сл. 8. Постојећи температурни модел на дан 16. мај 2019. (Ландсат 8, ТИР 10 и 11)

Tab. 2 (LST) The existing temperature model on May 16, 2019 (Landsat 8, TIR 10+11)/Таб. 2 (*LST*) Постојећи температурни модел на дан 16. мај 2019. (Landsat 8, TIR 10+11)

EXISTING LAND SURFACE TEMPERATURE ANALYSED ON THE BLOCK									
29	31	32	33	34	38	40	41	42	43
0	0	0	0	0	0	35,967	309,317	117,793	6,294
Total area: 469,371m²; **Average temp: 41.20**°C									

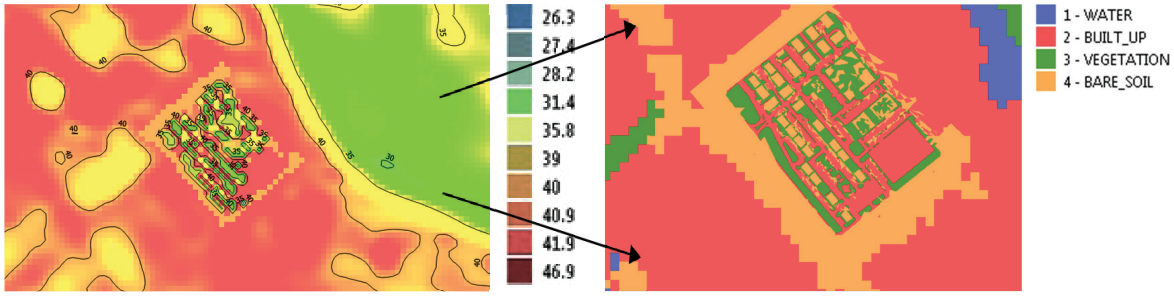

Fig. 9a (left) Thermal map (prediction model); Fig. 9b (right) Using new LULC classification as a base layer. / Сл. 9а (лево) Термална мапа (пројектовани модел); Сл. 96 (десно) Коришћење нове ЛУЛЦ класификације као базне подлоге.

Fig. 10a (left) Prediction model 1 (green buildings), Fig. 10b (right) Prediction model 2 (more greenery than in model 1) / Сл. 10а (лево) Пројектовани модел 1 (зелене зграде), Сл. 106 (десно) Пројектовани модел 2 (увећане зелене површине у односу на модел 1).

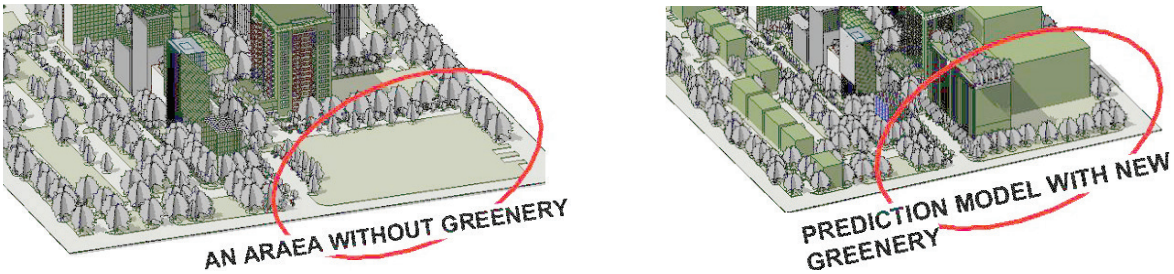

CLASS/Temp	29	31	32	33	34	38	40	41	42
BUILT-UP	151	151	2,279	1,979	852	1,311	7,123	17,199	6,918
URB. FOREST	60	65	2,776	2,963	4,351	3,187	3,670	5,629	1,246
MIX	8	3	3,485	2,065	1,367	3,385	22,064	12,945	3,083
SUM m^2	219	219	8,540	7,007	6,569	7,883	32,856	35,773	11,247
Average Temp	**38.92 ˚C**								
Total Area	**110,315 m^2**								

Tab. 3 Report for the average LST classification for prediction model 1 / Таб. 3 Извештај за просечну *LST* класификацију за пројектовани модел 1

Tab. 4 Report for the average LST classification for prediction model 2 / Таб. 4 Извештај за просечну *LST* класификацију за пројектовани модел 2

CLASS/Temp	29	31	32	33	34	38	40	41	42
BUILT-UP m	149	645	2,699	3,409	6,322	6,065	6,072	5,593	5,674
VEGETATION	308	1,813	5,178	5,359	4,698	4,075	3,006	1,840	202
MIX	21	303	4,063	7,992	7,819	8,266	8,787	7,490	1,960
SUM	491	2,792	11,971	16,794	18,872	18,444	17,904	14,963	7,893
Average Temp.	**36.70˚C**								
Total area	**110,124m^2**								

The green areas detected on the satellite images near the water bodies show more than 10˚C lower temperatures. The urban forest, well irrigated and integrated into the urban block, improved the quality of the urban climate and reduced the UHI. The greenery that was detected with a high evaporative factor in the given environment could not be identified regarding its type and species using the available method. The author could only guess whether these were artificial plantations for which watering was provided, or whether they were natural wild vegetation. Regardless of that fact, however, the typology of vegetation must belong to the class of high evaporative potential[7].

7 Palm trees, regardless of the fact that they belong to that climatic zone due to their reduced evaporation and shading, cannot be the right choice. In this desert climate from mid-November to mid-February, the days are shorter, and the exposure to sunlight is lower; therefore, in order to increase the thermal inertia and solar yield, it is considered that about 70% deciduous and about 30% evergreen vegetation would give a good result (under adequate irrigation) throughout the year.

Comparative results of the temperature impact on the reduction of thermal islands

The research results in prediction mode 1 (Fig. 10a), with fewer green buildings, and prediction model 2 (Fig. 10b), with more greenery, show a decrease in the LST (land surface temperature) as iterations from **41.2** to **36.70˚C** (the temperature difference between the models is **4.5˚C**) on an area of 11.1ha. The numerical results are shown in the report for the average LST classification for the prediction model (Tab. 3 and Tab. 4) for Fig. 10a and Fig. 10b, which means less need for fossil energy consumption, and less sulphur dioxide (SO^2) and carbon dioxide (CO^2) for Abu Dhabi's citizens.

The tables show the temperature changes in relation to the greenery, namely healthy vegetation (Fig. 10, Tab. 3 and Tab. 4) and the possibility of a reduction in urban heat islands (UHI) in a more sustainable way, i.e., a nature-based solution.

Fig. 11a Concept of watering urban infrastructure, Fig. 11b Roof water tank / Сл. 11а Урбани инфраструктурни концепт вештачког наводњавања, Сл. 11б Кровни резервар за воду

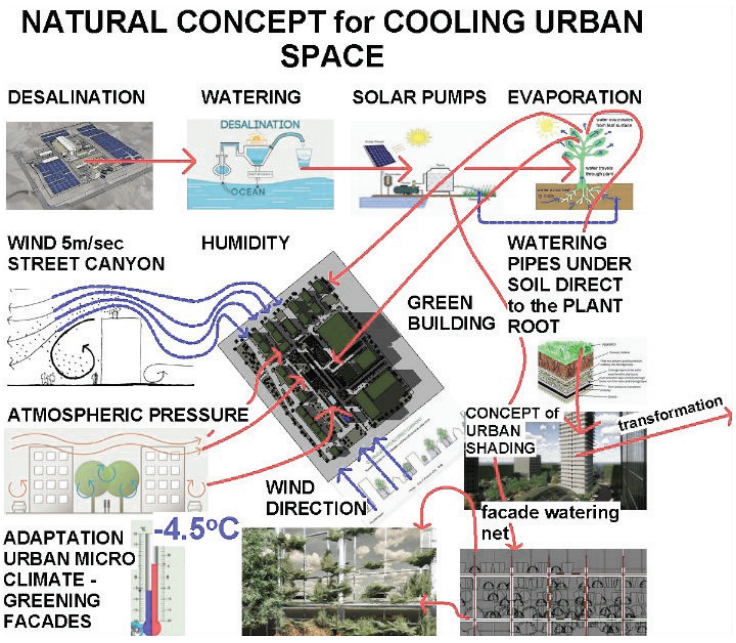

A natural concept for cooling urban space implies that it is a permanent thermodynamic process. In order for the plants to be able to evaporate, watering is necessary, without evaporation there is no cooling (Fig. 11a and Fig. 11b).

QUANTIFICATION OF THE IMPACT OF HIGH-RISE BUILDINGS ON GENERATING THERMAL HEAT ISLANDS

This study demonstrates how the energy consumption of buildings is composed, and its relation to the surrounding environment, the urban context, and the local variations of the microclimate. The results of this paper can be used in urban planning to improve the sustainability of new districts. The ratio of each building in the block model is relevant to the distribution of solar radiation for energy emission.

The following urban morphology factors (Mutani et al., 2016) were selected as being relevant for the change in the energy consumption of buildings within urban bloks:

- BCR building coverage ratio [m2/m2]
- BD building density [m3/m2]
- BH building height [m]
- H/W aspect ratio
- MOS main orientation of streets
- A albedo

Each of the factors was calculated based on the interrelationships of the buildings' geometry, the properties of the façade cladding and the assumed demographic density for a typical urban block in the city of Abu Dhabi.[8]

The urban characteristics of the buildings were calculated using EcoTech software. The results are shown in figs 12, 13 and 14. The block scale shows how energy consumptions vary as a function of the urban morphology and the solar exposure of outdoor spaces and daily shading. Moreover, solar exposure strongly influences energy consumption, especially for high building densities.

In the Abu Dhabi model, the reflected energy of the solar peak incident radiation on the roofs was about 900 W/h/m2 without greenery. With greenery it was 813 W/h/m2, a reduction of 87 W/h/m2. The test results supported by the GIS analysis have proven that the building envelope, depending on its properties and position, influences the reflection of gravitational LST and is inversely proportional to the evaporative potential and the surface of the vegetative cover.

Energy model explanation

There is a significant difference between façades with and without vegetation envelopes for the peak incident radiation (Fig. 13 and Fig. 14):

- roof 900 Wh/m^2; roof with vegetation 813 Wh/m^2
- southern 550 Wh/m^2; southern with vegetation 294 Wh/m^2
- west 391 Wh/m^2; west with vegetation 218 Wh/m^2
- east 365 Wh/m^2, east with vegetation 201 Wh/m^2

Through this model, it was found that the reflected energy of the solar radiation from the actual façade caused the temperature of the environment surrounding it to increase by about 2 to 6˚C.

The model shows that a significant proportion of vegetation can mitigate the reflective effect, such as the incident solar, direct, and diffuse solar radiation falling on objects. The solar

8 The building coverage ratio (BCR) is the ratio between the area of the buildings and the total area of the census section. The value can range from 0 without buildings, to 1 with an area fully covered with buildings. The building density (BD) is a product of the BCR and the building height (H, the average building height in the census section), which represents the ratio between the built volume and the surface of the area analysed (BD is proportional to the Floor Area Ratio FAR). The aspect ratio (H/W) is given by the ratio between the height of a building H and the distance between the buildings W; this parameter is used to generally evaluate the canyon effect (not important for single towers like the one in the example). The main orientation of the streets (MOS) represents the solar exposure of the city at urban block scale; with a prevailing east-west exposure, solar gains are greater, so the MOS factor assumes the maximum value of 1.5; while with a north-south exposure, solar gains are minimal and MOS is equal to 0.7. Finally, the albedo (A) of a surface is the reflected fraction of the incident radiation. The albedo depends on the type of materials but, for the same material, A is influenced by the wavelength and the incident angle of the radiation. The highest value of albedo is 1, when it is totally reflected; 0 is the minimum value with complete absorption.

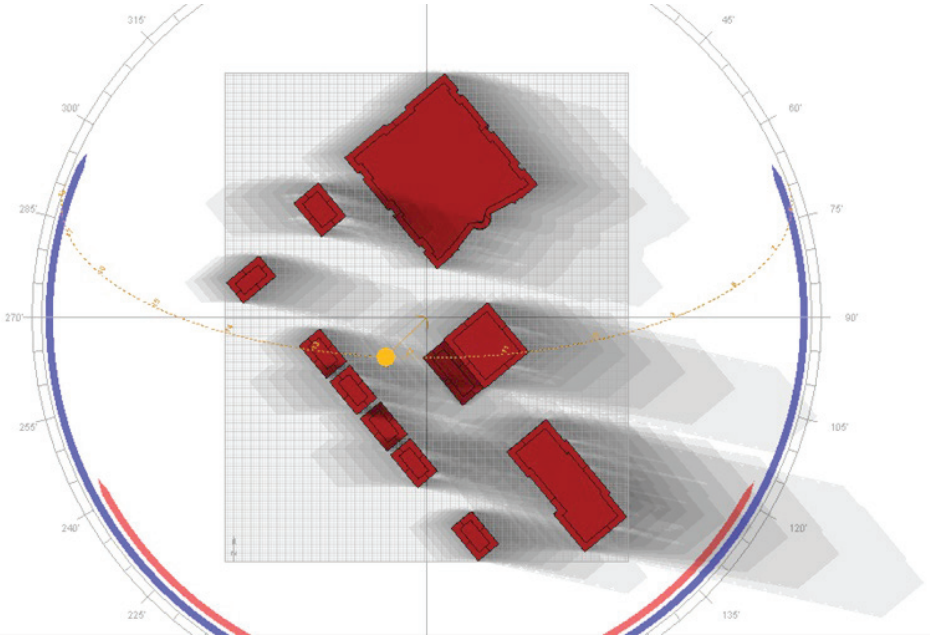

Fig. 12 Daily shading
Сл. 12 Дневно засенчење

radiation that is absorbed and transmitted, which is dependent on the surface material, was also calculated. In this case, the plain roof surface partly transmitted direct solar radiation by 41%: southern façades – 22%, west –19%, east –15%, and north-west – 3% per m^2. For instance, the façades of the tower on the north side of the model (a 62.2m high-rise) participate during the 8 hours of daylight with about 267.4 kWh (43Wh/m^2) of transmitted solar energy and with 18.5 Wh/m^2 of absorbed energy. Every building in the model is dependent on the position, surface area, volume, and type of envelope[9] and it increases the surrounding temperature by more than 4˚C.

THE NEW URBAN CONCEPT

Geospatial analyses were used to contribute to the effectives of the design for the new shape of the city block in Abu Dhabi. The basic concept of this study is that buildings and their outdoor water-green infrastructure make up an integral urban system necessitating co-current and simultaneous design solutions. The impact of the type of land cover was analysed. Both a statistical analysis of the results and an analysis of the changes in the surface temperature in a new urban model were performed (Fig. 15), as shown in the competition. A visual land-cover classification was drawn up, and used for the division of the territory into parcels, blocks and zones (for urban planning purposes). A detailed analysis of the data over the entire survey period shows the standard zones with urban heat islands which raise the city's temperature during the summer period. One of the conclusions of the study is that thermal images can be successfully used over time to detect changes in the land cover by temporal analysis.

Graphical design of the new urban concept-greening façades

The urban blue and green concept fully reflects the new model of the geospatial analysis. The streets are shaded with deciduous canopies; façades and roofs are also greened[10]. In front of the existing façades, a new spatial supporting structure with vegetation, fertile soil and irrigation system is formed. Urban green reconstruction applied to a block with healthy greenery positively affects climate change by reducing the LST by -4.5˚C as shown in the competition (Fig. 16).

9 Application of the principles : Rule book on Energy Efficiency of buildings (Official Gazette of RS, No. 61/2011)

10 Short video (*.mp4), a walkthrough of the new model can be seen on YouTube at: https://youtu.be/SaNH-E_dGKI

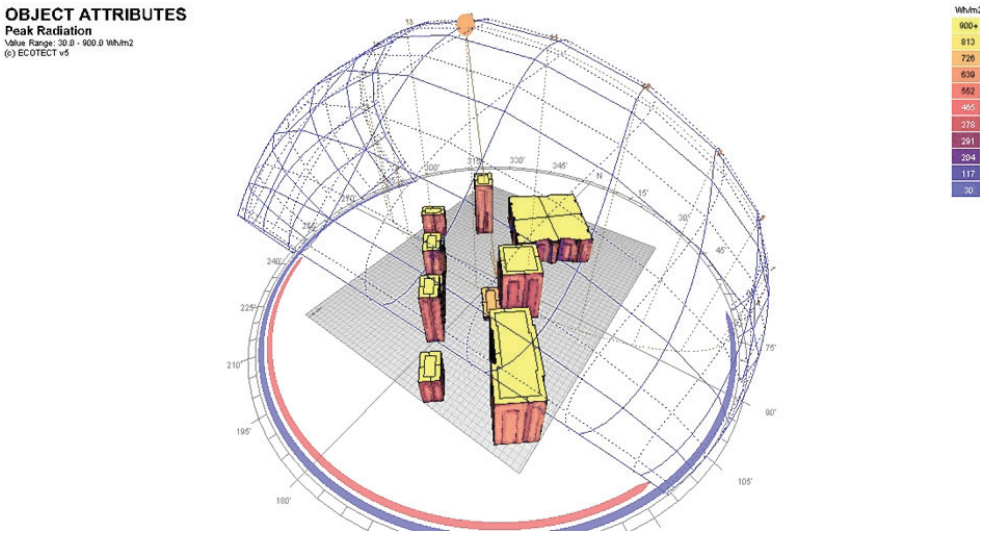

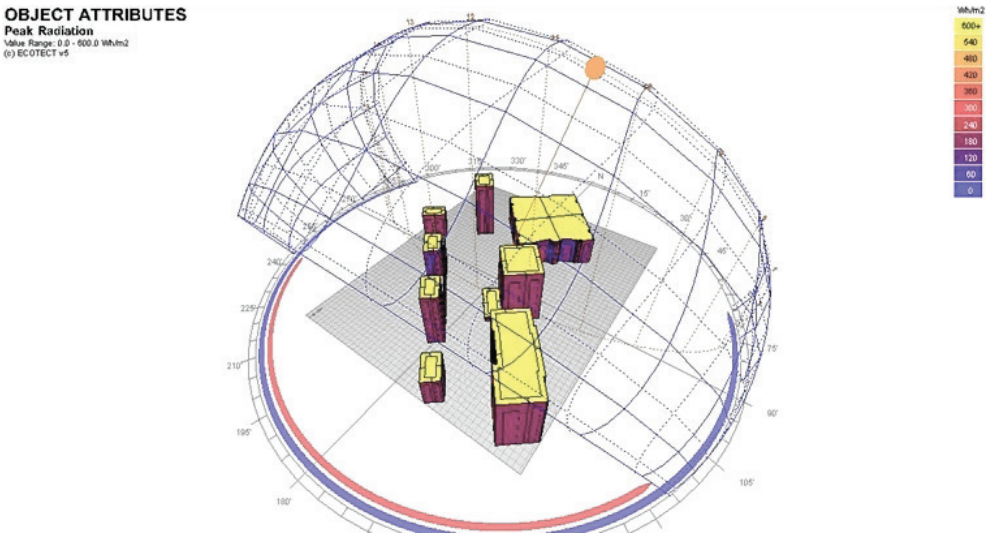

Fig.13. Peak façades without greenery cover
Fig. 14. Peak façades with greenery cover /
Сл. 13. Максимални дневни учинак за неозелењене фасаде
Сл. 14. Максимални дневни учинак за озелењене фасаде

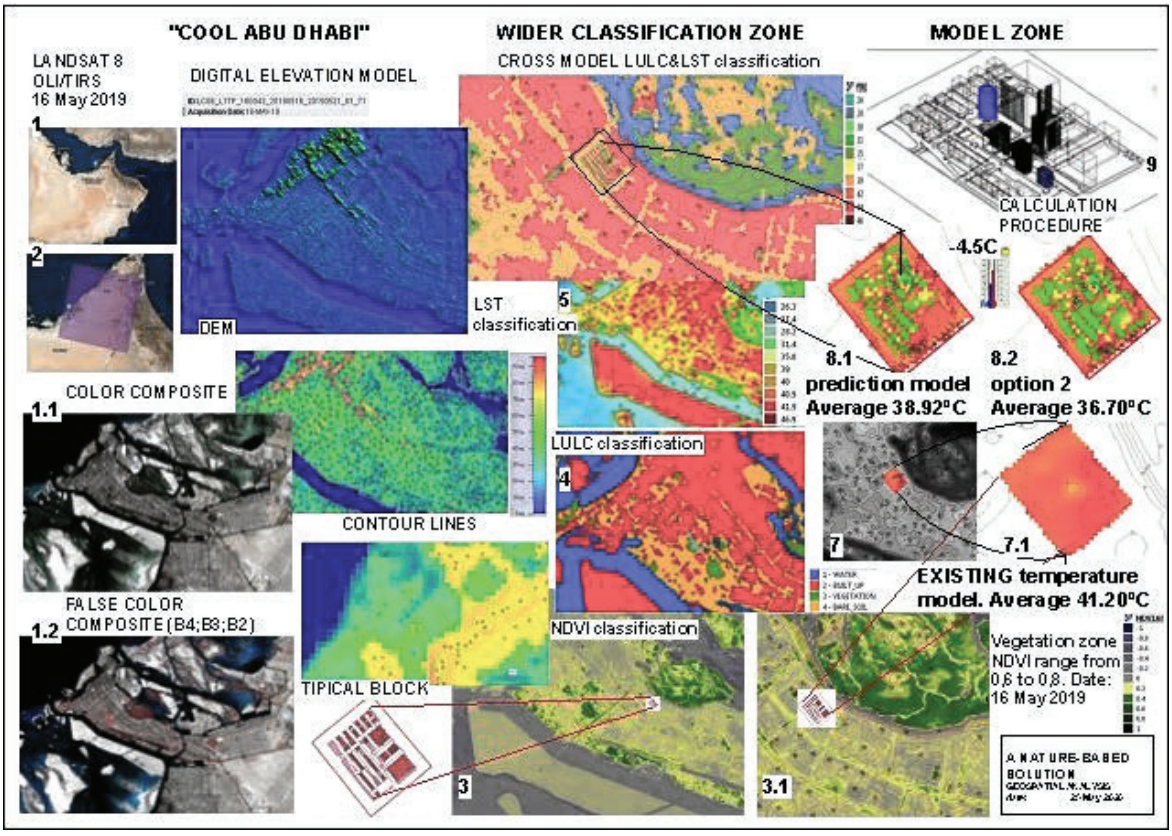

Fig. 15. Geospatial analysis / Сл. 15. Геопросторна анализа

SOCIAL IMPACT

Cities play a vital role in the quest to achieve global ecological sustainability. They are the largest contributors to greenhouse gases and climate change. However, if we manage to achieve the sustainable construction and use of urban infrastructure, they could likely become a critical leverage point in global efforts to drastically reduce emissions and avoid social and economic costs associated with climate change, as well as to enhance energy security and resilience in the face of high fossil energy prices.

Therefore, one of the critical priorities for big, modern cities, such as Abu Dhabi, is to encourage more energy-efficient developments. To this purpose, new buildings ought to be designed differently. For example, developers should make more use of natural passive cooling in the summer seasons, and they should implement only the most productive urban plans. The result should enable decision-makers (city governments) and urban planners to bring planning acts into line with the stated goals for climate change mitigation. Applied to Abu Dhabi, a tabular analysis of classes could be merged with individual parcels and zones and the results of the analysis covering broader areas of the city.

CONCLUSION

The test results support the notion that the building envelope, depending on its properties and position, influences the generation of the gravitational LST and is inversely proportional to the evaporative potential on the surface of the vegetative cover, resulting in a reduction in the area of urban heat islands.

Healthy vegetation has the evaporative cooling potential that can affect the microclimate of the Nature-based Solution.

The definition of a sustainable city is that it provides people with a high quality living environment without using huge amounts of natural resources (fossil fuels). Sustainability involves finding ways to design cities which are good places to live in, as well as being more efficient.[11] Designers and urbanists are also aware of the UN's upcoming 17 sustainable development goals. Goal number 11 is to make cities and human settlements inclusive, safe, resilient and sustainable.

For all the stakeholders – urban planners and decision-makers (local governments) – it is essential to have tools which would enable them to take concrete actions and create urban policies to further control LULC, in order to minimize its negative impacts, and to have a more balanced approach to influencing the microclimate of urban areas.

When buildings and their infrastructure are well balanced with water bodies and greenery in the surrounding area, their correlation is such that it enables an acceptable level of living and heating comfort and reduces the use of fossil fuels for cooling the urban area. By implementing remote sensing it is possible to analyse and quantify the impact of over-building on the rise in temperature in urban areas, as well as the disturbance of heating comfort and the increasing demands for additional cooling. Future predictions are modelled in this study as an example of good practice. The model is designed to be compatible with detailed urban plans (for each parcel, block or zone). By merging LULC and LST classified layers with land use register official layers in the appropriate scale, urban planners can synthesize the results for any parcel (plot) in the urban area in their land-use planning.

11 UN Habitat

Fig. 16 Future city concept / Сл. 16. Концепт будућег града

One of the key priorities for cities is to encourage a more energy efficient urban environment. This can be done by requiring new buildings to be designed in different ways, for example to make more use of natural passive cooling in the summer season and implementing the most productive, nature-based urban plans.

Another feature of this study is the presentation of relatively new GIS tools through the application of remote sensing methods, which simplified and enabled efficient networking of the data and classification by multiple criteria, as well as data analysis and proposing measures for remediating urban space. By defining an improved quality of life and creating visions of sustainable lifestyles (better comfort), it will be possible to outline how to design, support and govern a more sustainable city, where people could have a more comfortable life. An intelligently designed city can respond to the significant environmental, social, and economic challenges of the 21st century.

REFERENCES

Alshaikh A. (2015). Vegetation Cover Density and Land Surface Temperature Interrelationship Using Satellite Data, Case Study of Wadi Bisha, South KSA. Advances in Remote Sensing, 4, pp. 248-262.

Bannari A., Morin. D., Bonn F. (1995). A Review of Vegetation Indices. Remote Sensing Reviews,Vol.13 (1), pp. 95-120.

Đorđević T., Potić, I., Milanović, M. (2019). Quantification of the Impact of High-rise Buildings on Generating Heat Islands in the Area of the Realisation of the Special Purpose Plan 'Belgrade Waterfront' in Belgrade. In: Mihajlović, M. (Ed.) Environmental impact of illegal construction, poor planning and design IMPEDE 2019, Conference Proceedings, Belgrade, Association of Chemists and Chemical Engineers of Serbia (UHTS), pp. 376-387.

Garbulsky, M.F., Penuelas, J., Gamon, J., Inoue, Y., Fiella, I. (2011). The photochemical reflectance index (PRI) and the remote sensing of leaf, canopy, and ecosystem radiation use efficiencies: A review and meta-analysis. Remote Sensing of Environment, Vol.15 (2), pp.281-297.

Kalma J.D., McVicar T.R., McCabe, M.F. (2008). Estimating Land Surface Evaporation: A Review of Methods Using Remotely Sensed Surface Temperature Data. Survey in Geophysiscs, 29, pp.421-469.

Kojović M. (2013). Lokalne zajednice u održivom razvoju. Beograd: Evropski centar za mir i razvoj (EPCD) Univerziteta za mir Ujedinjenih nacija.

Milanović, M., Filipović, D. (2017). Informacioni sistemi u planiranju i zaštiti prostora. Beograd: Univerzitet u Beogradu - Geografski fakultet.

Mutani, G., Gamba, A., Maio, S. (2016). Space heating energy consumption and urban form. The case study of residential buildings in Turin (Italy). In: Ban, M. et al. (Eds.) Digital Proceedings of the 11th Conference on Sustainable Development of Energy, Water and Environment Systems, Lisbon, Zagreb: Faculty of Mechanical Engineering and Naval Architecture, SDEWES2016.0441, 1-17.

Noyingbeni K., Singh, P., Singgh, S., Vyas, A. (2016). Assessment of urban heat islands (UHI) of Noida City, India using multi-temporal satelite data. Sustainable Cities and Society, Vol. 22, pp. 19-28.

Yuan F., Bauer, M. (2007). Comparison of impervious surface area and normalized difference vegetation index as indicators of surface urban heat island effects in Landsat Imagery. Remote Sensing of Environment, Vol. 106(3), pp. 375-386.

SOFTWARE USED:

1. QGIS 3.x.x; 2. EcoTech 2011; 3. Arc Map 10.x; 4. Revit;5. Goole Earth Pro.
* All applications are open source or student's version.

ILLUSTRATIONS:

Fig. 1 https://www.coolabudhabi.com/challenge
Fig. 2 https://www.coolabudhabi.com/challenge
Fig. 3 https://www.usgs.gov/land-resources/nli/landsat
Fig. 4 source: author
Fig. 5 source: author
Fig. 6 source: author
Fig. 7a source: author; Fig.7b Google earth image
Fig. 8 https://www.usgs.gov/land-resources/nli/landsat
Fig. 9a source: author; Fig. 9b source: author
Fig. 10a source: author
Fig. 11a source: author; Fig. 11b source: author
Fig. 12 source: author
Fig. 13 source: author
Fig. 14 source: author
Fig. 15 source: author
Fig. 16 source: author